Binary phase shaping for selective single-beam CARS spectroscopy and imaging of gas-phase molecules

Paul J. Wrzesinski,[a]* Dmitry Pestov,[a] Vadim V. Lozovoy,[a] Bingwei Xu,[b] Sukesh Roy,[c] James R. Gord[d] and Marcos Dantus[a,b]

We report on mode-selective single-beam coherent anti-Stokes Raman scattering spectroscopy of gas-phase molecules. Binary phase shaping (BPS) is used to produce single-mode excitation of O_2, N_2, and CO_2 vibrational modes in ambient air and gas-phase mixtures, with high-contrast rejection of off-resonant Raman modes and efficient nonresonant-background suppression. In particular, we demonstrate independent excitation of CO_2 Fermi dyads at $\sim$1280 and $\sim$1380 cm^{-1} and apply BPS for high-contrast imaging of CO_2 jet in ambient air. Copyright © 2010 John Wiley & Sons, Ltd.

Keywords: pulse shaping; selective excitation; pseudorandom binary phase; standoff detection; spectroscopy

Introduction

Recent advances in pulse shaping and ultrafast laser technologies have brought coherent nonlinear optical techniques toward an outstanding level of laser-field control and functionality. Starting with the early work by Nelson and Weiner on pulse-sequence generation for enhanced impulsive stimulated Raman scattering in solids,[1,2] the use of pulse shapers has led to a variety of novel nonlinear optical techniques. Single-beam (single-pulse) coherent anti-Stokes Raman scattering (CARS) spectroscopy, first demonstrated for microscopy,[3] is one prominent example.

CARS is a third-order process that relies on coherent excitation of Raman active molecular vibrations.[4] The molecules are excited via pump and Stokes fields. The induced oscillations are then probed by a third laser pulse. The traditional implementation involves three laser beams of at least two different wavelengths that are overlapped in a phase-matched BOXCAR geometry and properly timed. In single-beam CARS, the pump, Stokes, and probe components are encompassed within a single broadband laser spectrum. Pulse shaping is then utilized to implement various strategies for background suppression, signal enhancement, and excitation selectivity if needed.

In their original work on single-beam CARS, Dudovich et al.[3] used a sinusoidal phase modulation both to gain selectivity and to suppress the nonresonant contribution. Silberberg's group also showed that a simple π-phase gate can give a certain degree of discrimination between the resonant and nonresonant contributions to the CARS spectra.[5] They soon followed with a demonstration of a phase-and-polarization shaping technique, which offered superior nonresonant-background suppression while preserving the multimode character of impulsive Raman excitation.[6] Another way of using both phase and polarization control was devised by Leone's group,[7] who employed the homodyne mixing of the resonant signal with the nonresonant background to improve the detection limit. This was followed with a heterodyne detection scheme for single-beam CARS by von Vacano et al.[8] Note that, due to both phase-matching

considerations (relaxed phase-matching constrains under high-NA focusing) and the lack of high-power sub-10-fs laser sources, the original focus of single-beam CARS techniques was microscopy. Dantus's group was the first to transfer this technology for standoff detection of vapors, liquids, and powdered samples.[9,10] It was also found valuable for CARS spectroscopy of combustion-related gases.[11]

As pointed out above, selective excitation of Raman modes facilitates nonresonant-background suppression in the single-beam CARS scheme. Importantly, it also allows elimination of multichannel acquisition of CARS spectra, which is difficult to integrate with high-speed laser beam scanning for imaging applications. The aforementioned sinusoidal phase modulation, though conceptually simple, provides a fairly low degree of signal rejection at off-resonant Raman frequencies. Better contrast is expected for linearly chirped pulses that have been utilized extensively in multibeam CARS setups.[12–14] Another attractive alternative, discussed in this work, is pseudorandom binary sequences. Using pseudorandom binary phase shaping (BPS), we have demonstrated previously high-contrast excitation selectivity for second-harmonic generation, two-photon excited fluorescence, and stimulated Raman scattering.[15] We have also applied BPS for mode-selective CARS in liquid samples.[9] Here we extend it to selective excitation of gas-phase molecules. In particular, we use pseudorandom BPS

---

* Correspondence to: Paul J. Wrzesinski, Department of Chemistry, Michigan State University, East Lansing, MI 48824, USA. E-mail: paul.wrzesinski@gmail.com

a Department of Chemistry, Michigan State University, East Lansing, MI 48824, USA

b BioPhotonics Solutions, Inc., 1401 East Lansing Drive, Suite 112, East Lansing, MI 48823, USA

c Spectral Energies, LLC, 5100 Springfield Street, Suite 301, Dayton, OH 45431, USA

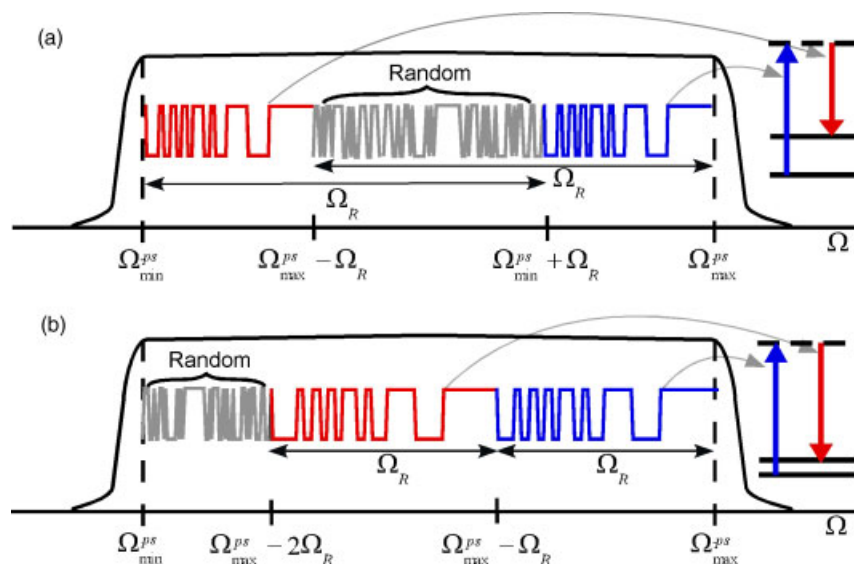d Propulsion Directorate, Air Force Research Laboratory, Wright-Patterson AFB, OH 45433, USA

Figure 1. Selective excitation of Raman active vibrational modes via BPS: (a) binary phase mask design for $\Delta\Omega^{ps} < 2\,\Omega_R$; (b) binary phase mask design for $\Delta\Omega^{ps} \geq 2\Omega_R$. Here $\Delta\Omega^{ps}$ is the bandwidth of the pump Stokes part of the laser spectrum; Ω_R is the transition Raman shift.

for selective excitation of O_2 ($\sim$1550 cm^{-1}) and N_2 ($\sim$2330 cm^{-1}) vibrations in ambient air. We also show independent excitation of CO_2 Fermi dyads at $\sim$1280 and $\sim$1380 cm^{-1} in gas-phase CO_2 and CO_2/N_2 mixtures. Finally, we demonstrate selective single-beam CARS imaging of CO_2 gas jet.

BPS for Selective Single-Beam CARS

Coherent vibrations of a molecular ensemble in CARS are established through the nonlinear interaction with the optical field. The excitation efficiency is, therefore, dependent on both the amplitude and the relative phase of contributing spectral components, or rather on multiphoton intrapulse interference since the excitation is impulsive.[16,17] The coherence amplitude at some wavenumber Ω_R is proportional to

$$E^{(0)}(\Omega_R) \equiv \int_0^{+\infty} E(\Omega + \Omega_R)E^*(\Omega)d\Omega \tag{1}$$

where $E(\Omega) \equiv |E(\Omega)| \exp[i\varphi(\Omega)] \propto \sqrt{S(\Omega)} \exp[i\varphi(\Omega)]$ is a complex spectral amplitude of the field at wavenumber Ω, determined by the spectral field intensity $S(\Omega)$ and phase $\varphi(\Omega)$. Since the pulse shaper operates with a finite number of independent channels, it is insightful to rewrite Eqn (1) for a mesh of N equidistantly spaced points between Ω_{min}^{ps} and Ω_{max}^{ps}:

$$E_n^{(0)} \equiv \sum_{m=0}^{N-n-1} E_{m+n}E_m^* \propto \sum_{m=0}^{N-n-1} \sqrt{S_{m+n}S_m} \exp[i(\varphi_{m+n} - \varphi_m)],$$
$$n = 0, \ldots, N-1 \tag{2}$$

The notations used are:

$$E_j^{(0)} = E^{(0)}(j\Delta\Omega_N), E_j \equiv E(\Omega_j), S_j \equiv S(\Omega_j), \varphi_j \equiv \varphi(\Omega_j),$$
$$\Omega_j = \Omega_{min}^{ps} + j\Delta\Omega_N, \Delta\Omega_N = (\Omega_{max}^{ps} - \Omega_{min}^{ps})/(N-1),$$
$$j = 0, \ldots, N-1 \tag{3}$$

If we now limit the phase values to 0 or π (more generally, to two values offset by π) and assume that the spectral intensity

within the $[\Omega_{min}^{ps}, \Omega_{max}^{ps}]$ interval remains constant, we find that the electric field $\{E_j\}$, subject to proper normalization, can be presented as a sequence of values $+1$ and -1. Since all such sequences of length M form a mathematical object known as a Galois field GF(2^M), the problem of selective excitation can be linked to the number theory problem of finding sequences of numbers $+1$ and -1 with minimal autocorrelation. Indeed, for every given Raman shift $\Omega_R^{j0} \equiv j_0\Delta\Omega_N$, the excitation efficiency is determined by $E_{j_0}^{(0)}$ from Eqn (2), i.e. by correlation of $\{E_j\}$ and $\{E_{j+j_0}\}$. When the binary sequence is repeated after Ω_R^{j0}, $E_j^{(0)}$ would have a maximum at $j = j_0$. The use of a minimal autocorrelation sequence to modulate the phase, however, ensures that the excitation at nearby frequencies is suppressed.[15]

Following the considerations above, the phase mask across the pump-Stokes part of the spectrum is built as follows (see the diagrams in Fig. 1). We first assign the minimal (Ω_{min}^{ps}) and maximal (Ω_{max}^{ps}) wavenumbers of the pump-Stokes band and compare its bandwidth ($\Delta\Omega^{ps} \equiv \Omega_{max}^{ps} - \Omega_{min}^{ps}$) with $2\Omega_R$, where Ω_R is the selected wavenumber. Here we assume that the pump-Stokes bandwidth $\Delta\Omega^{ps}$ exceeds Ω_R, i.e. the transition can be excited impulsively. If $\Delta\Omega^{ps} < 2\Omega_R$, as shown in Fig. 1(a), the chosen pseudorandom sequence is stretched over a ($\Delta\Omega^{ps} - \Omega_R$)-wide interval, from Ω_{max}^{ps} down to $\Omega_{min}^{ps} + \Omega_R$, and then repeated between $\Omega_{max}^{ps} - \Omega_R$ and Ω_{min}^{ps}, with translational symmetry relative to the first interval. The interval between $\Omega_{max}^{ps} - \Omega_R$ and $\Omega_{min}^{ps} + \Omega_R$, which does not contribute toward excitation at Ω_R, is filled with a high-frequency random binary phase to suppress the background contribution from this part of the spectrum. If $\Delta\Omega^{ps} \geq 2\Omega_R$ (Fig. 1(b)), the Galois sequence is stretched over Ω_R and encoded from Ω_{max}^{ps} to $\Omega_{max}^{ps} - 2\Omega_R$, and then from $\Omega_{max}^{ps} - 2\Omega_R$ down to $\Omega_{max}^{ps} - 2\Omega_R$. The leftover SLM pixels are again filled with a high-frequency random binary phase. In principle, one can put in as many sequence copies as can fit in $\Delta\Omega^{ps}$, i.e. more than 2. The extra copies, however, will contribute to higher harmonics of Ω_R as well. Finally, it is worthwhile to note here that Galois sequences are best suited for shaping of flat-top laser spectra. Their minimal autocorrelation property implies equally weighted contribution from every term in a sequence, which is not quite the case for
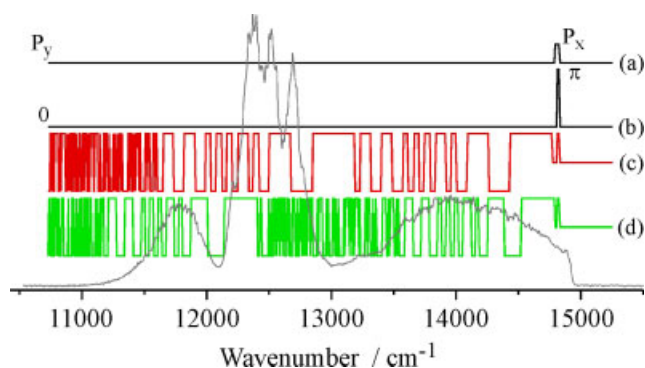
Figure 2. Phase and polarization shaping for multimode and selective single-beam CARS measurements. (a) Polarization mask encoded onto the laser spectrum, shown on the background by the gray line; (b) phase mask for multimode CARS measurements, when all Raman modes within the laser bandwidth are excited; (c and d) pseudorandom phase masks used for selective single-beam CARS from O_2 (1550 cm^{-1}) and N_2 (2330 cm^{-1}), respectively.

Figure 3. Calculated excitation spectra $\eta(\Omega_R)$ for a transform limited pulse (no phase modulation) and waveforms, produced by pseudorandom binary phase shaping for selective excitation at 1280, 1380, 1550, and 2330 cm^{-1}.

the spectrum provided by our laser source. In practice, it results in inferior background suppression when compared to the optimal case.

To retrieve CARS spectra, we use a polarization shaping technique.[6,9] The polarization of a narrow band on the blue side of the laser spectrum (polarization P_x in Fig. 2(a), four SLM pixels wide) is rotated by 90° relative to the remaining spectrum. The polarizer in the acquisition arm is also set along this polarization. Only CARS photons with polarization P_x are detected. The intense P_y-polarized signal, overwhelmed by the nonresonant background produced by the pump-Stokes component and having poor spectral resolution, is rejected. We also encode a π-phase step across the P_x-polarized band when acquiring multimode CARS spectra, as shown in Fig. 2(b). The π step is used to minimize the time overlap between the P_y-polarized pump-Stokes and P_x-polarized probe parts, mitigating the contribution due to the instantaneous electronic response.

Two examples of selective-excitation phase masks, based on a 37-bit Galois sequence, are shown in Fig. 2(c) and (d). The phase mask in Fig. 2(c) is designed to excite the O_2 vibrational mode at ~1550 cm^{-1}. For the given experimental parameters, the condition $\Delta\Omega^{ps} \geq 2\Omega_R$ is fulfilled; therefore, the Galois binary sequence is stretched over 1550 cm^{-1}, and its two copies are stacked together next to the probe band. The pseudorandom phase mask in Fig. 2(d) targets the N_2 Raman transition at ~2330 cm^{-1}. Here $\Delta\Omega^{ps} < 2\Omega_R$ and the two sequence copies are separated by a random binary modulation.

Using this method, phases for selective excitation of the two Fermi dyads of CO_2, and the Raman modes of O_2 and N_2 were designed. The normalized excitation efficiency spectra $\eta(\Omega_R)$,

$$\eta(\Omega_R) \equiv |E^{(0)}(\Omega_R)/E^{(0)}(0)|^2 \qquad (4)$$

for each of the phases as well as for zero phase, which corresponds to a transform limited (TL) pulse, are shown in Fig. 3. From the figure it is clear that BPS is used most effectively when the condition $\Delta\Omega^{ps} < 2\Omega_R$ is fulfilled. When $\Delta\Omega^{ps} \geq 2\Omega_R$, BPS eliminates high-harmonic contributions at the expense of the inferior excitation strength. Raman-shift-dependent excitation efficiencies, both due to the limited laser bandwidth and spectral phase shaping, contribute toward the strength of Raman peaks observed in CARS spectra. In principle, such dependences might
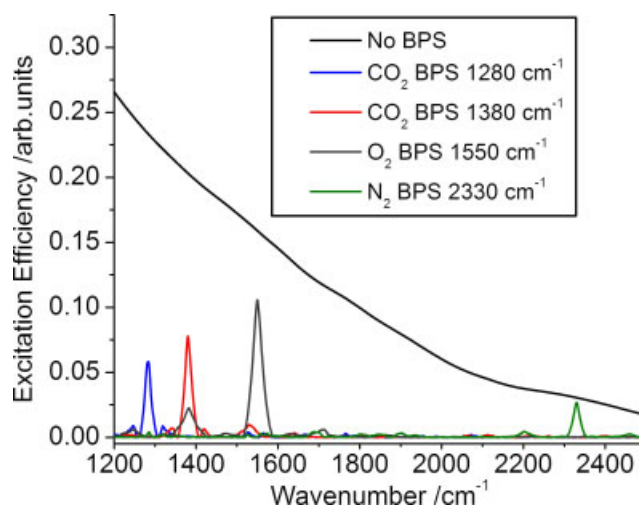
be accounted for experimentally by the normalization of the CARS signal on the purely nonresonant response from a reference sample. To predict the measured CARS spectra or use those to retrieve relative concentrations of contributing species, however, one also needs to account for the timing between the pump-Stokes and probe fields, Raman cross-sections of transitions being examined, and their coherence dephasing rates. This is currently under development, along with other possible methods to perform selective excitation in single-beam CARS.

Experimental Setup

The experiments were performed with a system based on a Ti : sapphire regenerative amplifier (Legend, Coherent Inc.) (Fig. 4). A pulse shaper (not shown) was installed between the oscillator (Micra, Coherent Inc.) and the amplifier to remove high-order phase distortion of laser pulses at the regenerative-amplifier output. The laser spectrum was then broadened through self-phase modulation in a hollow waveguide (HWG),[18] constructed from a 39-cm-long glass capillary with a core diameter of ~300 μm and filled with argon at ~2 bar. The HWG output bandwidth was optimized by varying the input power, pulse chirp, and argon pressure. The typical spectrum of a pulse reaching the sampled volume is shown in the inset of Fig. 1. The corresponding TL pulse duration is ~7 fs. Phase distortions of the pulse at the sample (primarily linear chirp of ~2000 fs^2) were corrected via multiphoton intrapulse interference phase scan (MIIPS),[19] performed with a 4f pulse shaper located after the HWG. The same shaper was used for polarization and phase shaping as discussed below. It had a dual-mask 640-pixel spatial light modulator (CRi SLM-640-D) at the Fourier plane, with the polarizer removed. The beam of shaped pulses was focused in ambient air or a gas pressure cell using a curved mirror of 75 cm focal length. A concave metallic mirror with 25 cm focal length was used for imaging of the CO_2 jet. The generated CARS signal was separated from the input field using a 650-nm short-pass filter (Omega Optics) and a calcite polarizing cube (Newport), with the transmission axis set perpendicular to the polarization of the excitation photons. The filtered CARS photons were either focused into a high-resolution
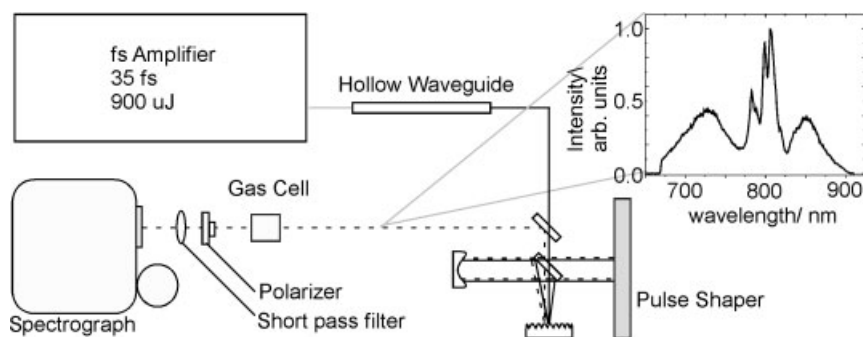
Figure 4. Schematic diagram of single-beam CARS experimental setup. SLM, spatial light modulator. Inset: a typical pulse spectrum at the sample.
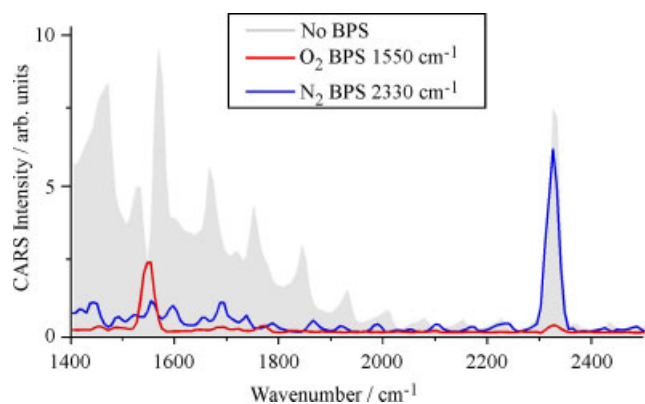

Figure 5. Selective single-beam CARS from O_2 and N_2 vibrations in ambient air.
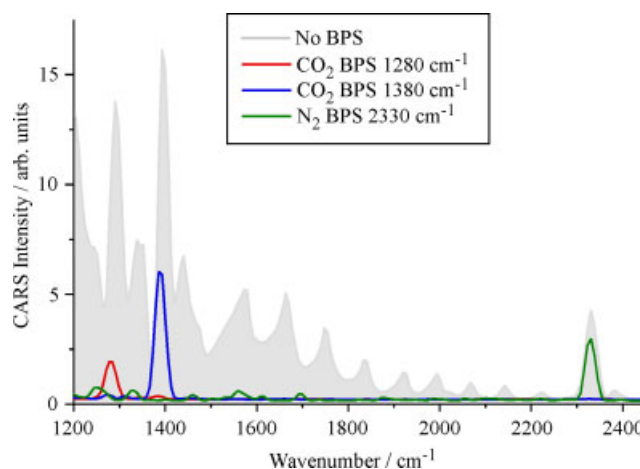

Figure 6. Selective single-beam CARS of a 1:1 N_2/CO_2 mixture at 1 atm pressure.

spectrograph with a liquid-nitrogen (LN) cooled CCD camera or fiber-coupled into a low-resolution Ocean Optics QE-65000 spectrometer. For imaging experiment, we used two motorized translation stages to shift the nozzle in the focal plane of the laser beam. Spectrally integrated CARS signal over 1460 cm^{-1} was recorded as a function of the nozzle position.

Results and Discussion

Selective excitation via BPS was examined with several different gases. Initial experiments were performed with ambient air, whose CARS spectrum is expected to have two strong Raman lines corresponding to vibrations of O_2 ($\sim$1550 cm^{-1}) and N_2 ($\sim$2330 cm^{-1}) molecules. The experimental multimode CARS spectrum (gray shadow in Fig. 5) indeed features a pronounced N_2 line. The O_2 line, however, is hidden by the remaining nonresonant contribution that rises at low wavenumbers. Selective excitation at 1550 cm^{-1}, using the phase mask from Fig. 2, mitigates the interfering background and makes the O_2 line obvious. The other pseudorandom phase mask highlights the N_2 vibrational mode. The slight offset of the spectra from zero is due to the electronic dark current of the LN-cooled CCD used for detection.

Single-beam CARS measurements with a 1:1 N_2/CO_2 mixture in the pressure cell showed similar results. In the multimode CARS spectrum, the nonresonant background due to the instantaneous electronic response interferes with the two CO_2 signatures (Fig. 6). The designed binary phase masks allow the excitation of all three Raman lines, including the N_2 line and CO_2 Fermi dyads at $\sim$1280

and $\sim$1380 cm^{-1}, independently. They also strongly suppress the nonresonant background.

The excitation selectivity contrast can be inferred from Fig. 7(a), where the CARS signal intensities at 1280 cm^{-1}, 1380 cm^{-1} and over the entire spectral region (625–2125 cm^{-1}) from pure CO_2 gas at 1 atm are plotted as a function of the design parameter Ω_R. Several representative CARS spectra, acquired with Ocean Optics QE-65000 spectrometer while scanning Ω_R, are shown in Fig. 7(b). When the 1280 cm^{-1} line is selectively excited, the ratio of CARS intensities between the 1280 and 1380 cm^{-1} lines is 10:1. For selective excitation of the 1380 cm^{-1} CO_2 line, the ratio between the 1280 and 1380 cm^{-1} lines is 1:24. When the CARS signal is not resolved spectrally, the contrast is limited primarily by the cumulative nonresonant contribution reaching the detector.

To emphasize the utility of selective BPS, we imaged a jet of CO_2 gas, flowing out a narrow rectangular nozzle, with TL and shaped pulses. In both cases, a 0.6 × 2.2 mm region near the tip of the nozzle was scanned using 0.01-mm and 0.05-mm step sizes along vertical and horizontal axes, respectively. The spectrally integrated CARS signal from 1060 to 2520 cm^{-1} was recorded at each position in the scan. The image obtained with TL pulses (Fig. 8(a)) exhibits poor chemical contrast, which can be improved by spectral filtering of the CARS signal corresponding to the CO_2 lines or by post-processing of CARS spectra if those are available. Note that the CARS spectra over the observed range featured N_2 and O_2 lines from ambient air as well as comparable nonresonant contribution
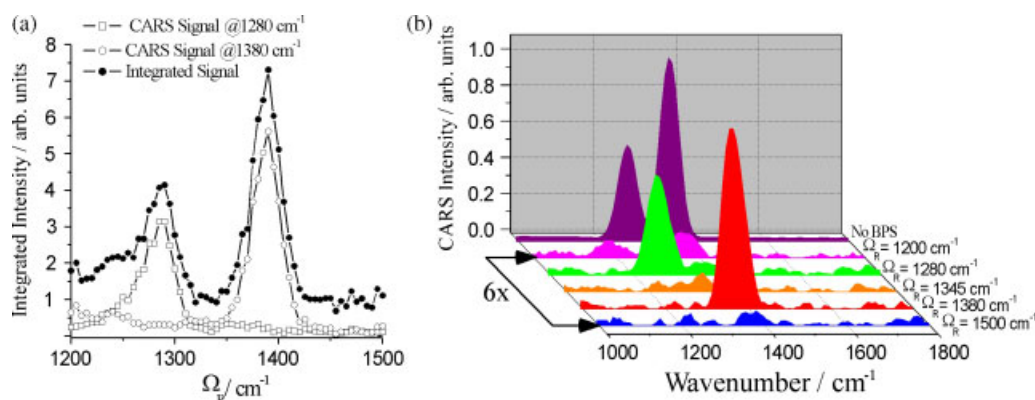
Figure 7. Selective single-beam CARS of pure CO_2 at 1 atm. The target Raman shift Ω_R of the pseudorandom binary phase is tuned through the two resonances with CO_2 Fermi dyads at ~1280 and ~1380 cm^{-1}. (a) CARS signal intensities at 1280 cm^{-1}, 1380 cm^{-1}, and integrated over 625–2125 cm as a function of Ω_R. (b) Experimental CARS spectra acquired for Ω_R equal to 1200, 1280, 1330, 1380, and 1500 cm^{-1} The multimode, single-beam CARS spectrum of CO_2 (no BPS) is shown as a reference. The other CARS spectra are scaled in intensity by a factor of 6.
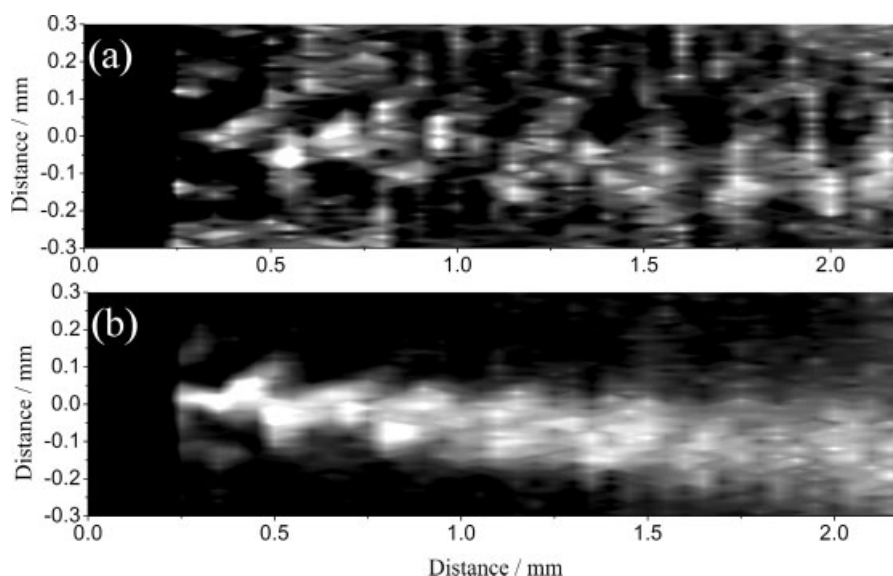

Figure 8. Imaging of a CO_2 gas jet with (a) no BPS and (b) BPS excitation at 1280 cm^{-1}.

at lower wavenumbers (longer wavelengths). Selective excitation, implemented in Fig. 8(b) for the 1280 cm^{-1} Raman transition in CO_2, virtually eliminates the need for signal post-processing, favors single-channel detection, and allows straightforward tuning between different Raman resonances. The image in Fig. 8(b) demonstrates excellent chemical contrast and reveals interesting dynamics of the turbulent CO_2 flow. In particular, the intensity modulation seen in the CO_2 flow is reproducible from image to image and is deemed to be characteristic of the imaged jet.

Conclusions

We have extended the pseudorandom BPS technique, introduced elsewhere, to selective excitation of high-wavenumber molecular vibrational modes in the gas phase. In particular, we have used it to address Raman transitions of O_2 and N_2 in ambient air as well as CO_2 Fermi dyads in a 1 : 1 N_2/CO_2 mixture and pure CO_2 gas at atmospheric pressure. We have shown that pulse phase shaping using pseudorandom BPS allows high contrast selectivity and

efficient nonresonant background suppression in single-beam CARS measurements, enabling high-contrast spectroscopy and imaging.

References

[1] A. M. Weiner, D. E. Leaird, G. P. Wiederrecht, K. A. Nelson, *J. Opt. Soc. Am. B: Opt. Phys.* **1991**, *8*, 1264.
[2] H. Kawashima, M. M. Wefers, K. A. Nelson, *Annu. Rev. Phys. Chem.* **1995**, *46*, 627.
[3] N. Dudovich, D. Oron, Y. Silberberg, *Nature* **2002**, *418*, 512.
[4] Y. R. Shen, *The Principles of Nonlinear Optics*, Wiley Classics Library ed., John Wiley &Sons, Inc.: Hoboken, New Jersey, USA, **2003**.
[5] N. Dudovich, D. Oron, Y. Silberberg, *J. Chem. Phys.* **2003**, *118*, 9208.

 wileyonlinelibrary.com/journal/jrs

[6] D. Oron, N. Dudovich, Y. Silberberg, *Phys. Rev. Lett.* **2003**, *90*, 213902.

[7] S. H. Lim, A. G. Caster, S. R. Leone, *Phys. Rev. A* **2005**, *72*, 041803.

[8] B. von Vacano, T. Buckup, M. Motzkus, *Opt. Lett.* **2006**, *31*, 2495.

[9] H. W. Li, D. A. Harris, B. Xu, P. J. Wrzesinski, V. V. Lozovoy, M. Dantus, *Opt. Express* **2008**, *16*, 5499.

[10] H. W. Li, D. A. Harris, B. Xu, P. J. Wrzesinski, V. V. Lozovoy, M. Dantus, *Appl. Opt.* **2009**, *48*, B17.

[11] S. Roy, P. Wrzesinski, D. Pestov, T. Gunaratne, M. Dantus, J. R. Gord, *Appl. Phys. Lett.* **2009**, *95*, 074102.

[12] E. Gershgoren, R. A. Bartels, J. T. Fourkas, R. Tobey, M. M. Murnane, H. C. Kapteyn, *Opt. Lett.* **2003**, *28*, 361.

[13] T. Hellerer, A. M. K. Enejder, A. Zumbusch, *Appl. Phys. Lett.* **2004**, *85*, 25.

[14] D. Pestov, X. Wang, R. K. Murawski, G. O. Ariunbold, V. A. Sautenkov, A. V. Sokolov, *J. Opt. Soc. Am. B: Opt. Phys.* **2008**, *25*, 768.

[15] V. V. Lozovoy, B. W. Xu, J. C. Shane, M. Dantus, *Phys. Rev. A* **2006**, *74*, 041805.

[16] K. A. Walowicz, I. Pastirk, V. V. Lozovoy, M. Dantus, *J. Phys. Chem. A* **2002**, *106*, 9369.

[17] V. V. Lozovoy, M. Dantus, *ChemPhysChem* **2005**, *6*, 1970.

[18] M. Nisoli, S. DeSilvestri, O. Svelto, *Appl. Phys. Lett.* **1996**, *68*, 2793.

[19] Y. Coello, V. V. Lozovoy, T. C. Gunaratne, B. W. Xu, I. Borukhovich, C. H. Tseng, T. Weinacht, M. Dantus, *J. Opt. Soc. Am. B: Opt. Phys.* **2008**, *25*, A140.